



Supplement of

Evolution of atmospheric age of particles and its implications for the formation of a severe haze event in eastern China

Xiaodong Xie et al.

Correspondence to: Jianlin Hu (jianlinhu@nuist.edu.cn)

The copyright of individual parts of the supplement might differ from the article licence.

Contents of this file

Text S1

Table S1-S3

Figures S1–S20

Text S1. Model evaluation

Evaluation of WRF-simulated meteorological parameters in the NCP and the YRD during this haze episode is shown in **Figure S2**. The corresponding mean bias (MB), mean error (ME), root mean square error (RMSE), correlation coefficient (R), and index of agreement (IOA) were calculated and summarized in **Table S3**. Compared with observations in both the NCP and the YRD, the WRF model captures well the magnitude and temporal variation of T_{2m} and RH with high correlation coefficients of 0.97–0.98, but slightly underestimates T_{2m} with MBs of -0.2 °C to -0.1 °C and overestimates RH with MBs of 0.5% to 2.6%. The simulated WS is underestimated with MBs of -0.35 m s⁻¹ to -0.26 m s⁻¹, especially for high wind speed conditions. The RMSEs of WS are less than 1 m s⁻¹ and the IOAs are larger than 0.7, which satisfy the benchmarks suggested by Emery et al. (2001). For WD, the MEs are less than 30° and the correlation coefficients are larger than 0.8, indicating the WRF model can capture the variations of wind direction during this haze episode. Overall, the simulated meteorological parameters in this study agree well with observations, and the model performance is comparable to other works using the WRF model in China (Chen et al., 2017a; Hu et al., 2016; Zheng et al., 2015a).

The UCD/CIT model performance of PM_{2.5} and its major chemical compositions in eastern China is evaluated. The UCD/CIT model well reproduces the observed temporal variations of hourly PM_{2.5} concentrations averaged over the NCP and the YRD during this haze episode with a high correlation coefficient ($R > 0.85$) and a low bias (NMB < 15%) (**Figure 2b**). High PM_{2.5} concentrations (> 150 µg m⁻³) with low wind speed over southern Hebei, Shandong, Henan, northern Jiangsu, and Anhui provinces are well captured by the model (**Figure S5**). The simulated PM_{2.5} compositions (SO₄²⁻, NO₃⁻, NH₄⁺, EC, and organic matter (OM)) also agree well with the daily-averaged measurements in Beijing, Jinan, Nanjing, and Shanghai (**Figure S6**), with model performance statistics comparable to those in other studies (Shi et al., 2017; Hu et al., 2016; Zhang et al., 2019b). The correlation coefficients of SO₄²⁻, NO₃⁻, and NH₄⁺ are found to be 0.80, 0.80, and 0.87 respectively, indicating that the UCD/CIT model successfully captures the day-to-day variations of secondary inorganic aerosols (SO₄²⁻, NO₃⁻, and NH₄⁺; hereafter referred to as SNA).

However, the model significantly underestimates SO_4^{2-} concentrations with an NMB of -42.3% , especially when the observed SO_4^{2-} concentrations are high. Underestimation of SO_4^{2-} has also been pointed out by many other modeling studies in China, which is mainly attributed to the missing mechanisms, such as heterogeneous chemistry, in current air quality models (Song et al., 2021; Zheng et al., 2015a; Wang et al., 2014). The model captures the observed NO_3^- concentrations well, with an NMB and NME of -7.8% and 33.1% respectively. The model performance of NH_4^+ is better than SO_4^{2-} but slightly worse than NO_3^- , and the NMB and NME values meet the performance criteria. The UCD/CIT model can generally capture the spatiotemporal variations of EC but has a positive NMB of 62.6% . The large overestimation of EC is mainly attributed to the uncertainties in emission inventory, which has also been found in previous studies (Zheng et al., 2015a; Wang et al., 2021d). Other reasons, such as the relatively coarse model grid resolution (36 km) and uncertainties in predicted meteorological parameters, may also contribute to this bias (Hu et al., 2016; Liu et al., 2020). The NMB and NME of OM meet the model performance criteria, indicating OM predictions agree well with measurements. Nevertheless, OM is slightly underestimated with an NMB of -6.3% . This is mainly attributed to the underestimations in SOA due to the missing formation pathways such as multigenerational aging of semi-volatile organic compounds, and heterogeneous and aqueous-phase pathways in current air quality models (Chen et al., 2017b; Hu et al., 2015).

Overall, the above evaluations suggest that the simulated meteorological parameters and particle concentrations are consistent with observations, verifying a good model performance in eastern China during this haze episode.

Table S1. Fractional apportionment of particle-phase emissions across the 15 size bins in the UCD/CIT model.

Size bin	Diameter (nm)	Emission fractions				
		Industry	Residential	Power	Transportation	Wildfire
1	<10	0	0.0001	0	0.0046	0.0000
2	10-16	0	0.0004	0	0.0103	0.0007
3	16-25	0	0.0019	0	0.0140	0.0046
4	25-39.5	0.0004	0.0104	0.0004	0.0284	0.0437
5	39.5-63	0.0239	0.0295	0.0239	0.0839	0.1632
6	63-100	0.2542	0.0931	0.2542	0.2617	0.2601
7	100-160	0.5139	0.2366	0.5139	0.2194	0.2637
8	160-250	0.1902	0.2756	0.1902	0.0970	0.1017
9	250-395	0.0172	0.2225	0.0172	0.0732	0.0379
10	395-630	0.0002	0.0727	0.0002	0.0680	0.0343
11	630-1000	0	0.0163	0	0.0145	0.0308
12	1000-1600	0	0.0409	0	0.0305	0.0260
13	1600-2500	0	0	0	0.0325	0.0162
14	2500-3950	0	0	0	0.0312	0.0081
15	3950-10000	0	0	0	0.0310	0.0091

Table S2. Average atmospheric age represented by each age bin for simulations with different age bin updating intervals. The grey-shaded cells indicate the results used in the final analysis.

Age bins	Age bin updating interval (h)				
	1	3	6	8	12
0	0.5	1.5	3	4	6
1	1.5	4.5	9	12	18
2	2.5	7.5	15	20	30
3	3.5	10.5	21	28	42
4	4.5	13.5	27	36	54
5	5.5	16.5	33	44	66
6	6.5	19.5	39	52	78
7	7.5	22.5	45	60	90
8	8.5	25.5	51	68	102

Table S3. Statistical evaluations of meteorological performance

	<i>OBS</i> ¹	<i>SIM</i> ¹	<i>MB</i> ²	<i>ME</i> ³	<i>RMSE</i> ⁴	<i>R</i> ⁵	<i>IOA</i> ⁶
NCP							
T _{2m} (°C)	-0.46	-0.61	-0.15	0.78	1.04	0.97	0.98
RH (%)	53.30	55.86	2.56	3.40	4.30	0.97	0.97
WS (m s ⁻¹)	2.47	2.12	-0.35	0.47	0.64	0.76	0.75
WD (°)	196.89	184.58	-12.31	20.73	37.57	0.95	0.97
YRD							
T _{2m} (°C)	6.55	6.45	-0.10	0.52	0.67	0.98	0.99
RH (%)	74.20	74.71	0.52	2.76	3.75	0.98	0.99
WS (m s ⁻¹)	2.39	2.13	-0.26	0.39	0.50	0.79	0.85
WD (°)	131.05	134.27	3.22	18.81	60.60	0.84	0.92

¹*OBS* and *SIM* represent the mean observed and simulated values from 25 December 2017 to 2 January 2018, respectively.

²*MB* is the mean bias, $MB = \frac{1}{N} \sum (SIM_i - OBS_i)$; *SIM*_{*i*} and *OBS*_{*i*} are hourly observed and simulated values. *N* is the total number of hours.

³*ME* is the mean error, $ME = \frac{1}{N} \sum |SIM_i - OBS_i|$.

⁴*RMSE* is the root mean square error, $RMSE = \sqrt{\frac{1}{N} \sum (SIM_i - OBS_i)^2}$

⁵*R* is the correlation coefficient, $R = \frac{\sum [(SIM_i - \overline{SIM}) \times (OBS_i - \overline{OBS})]}{\sqrt{\sum (SIM_i - \overline{SIM})^2 \times \sum (OBS_i - \overline{OBS})^2}}$.

⁶*IOA* is the index of agreement, $IOA = 1 - \frac{\sum (SIM_i - OBS_i)^2}{\sum (|SIM_i - \overline{SIM}| + |OBS_i - \overline{OBS}|)^2}$.

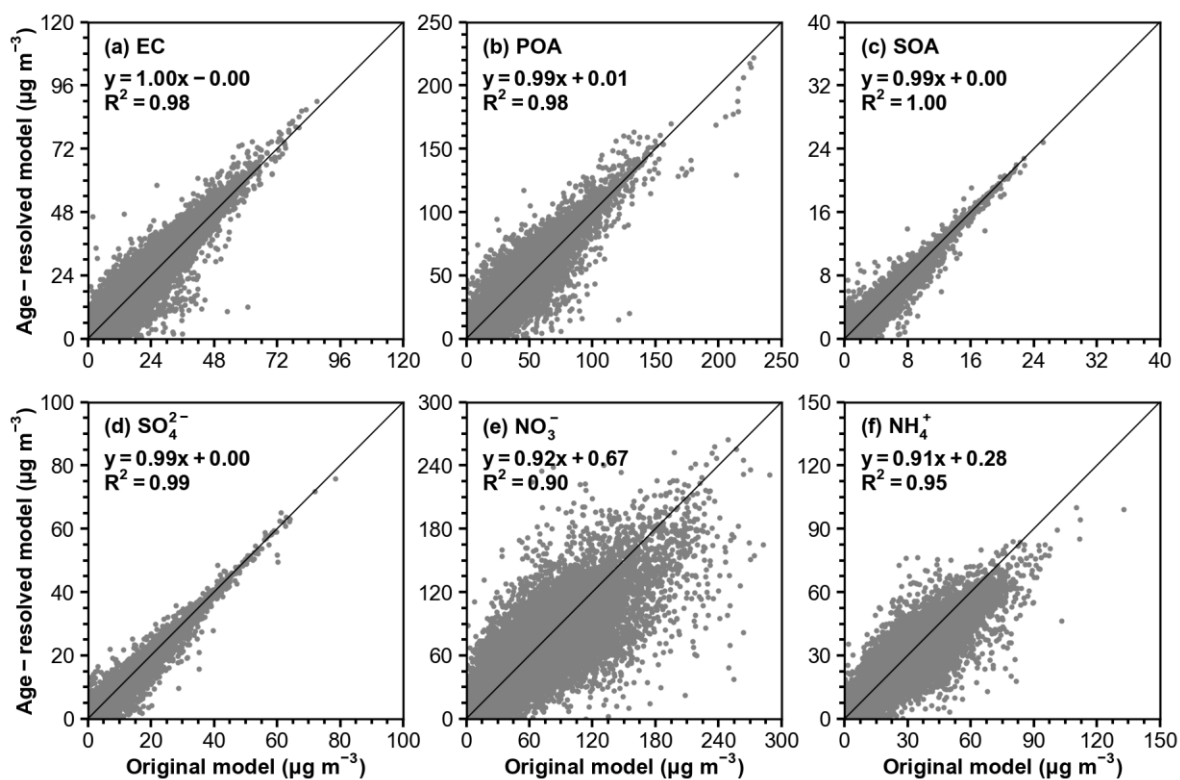


Figure S1. Comparison of EC, POA, SOA, SO_4^{2-} , NO_3^- , and NH_4^+ concentrations ($\mu\text{g m}^{-3}$) predicted by the age-resolved UCD/CIT model against the original UCD/CIT model for all grid cells within the model domain.

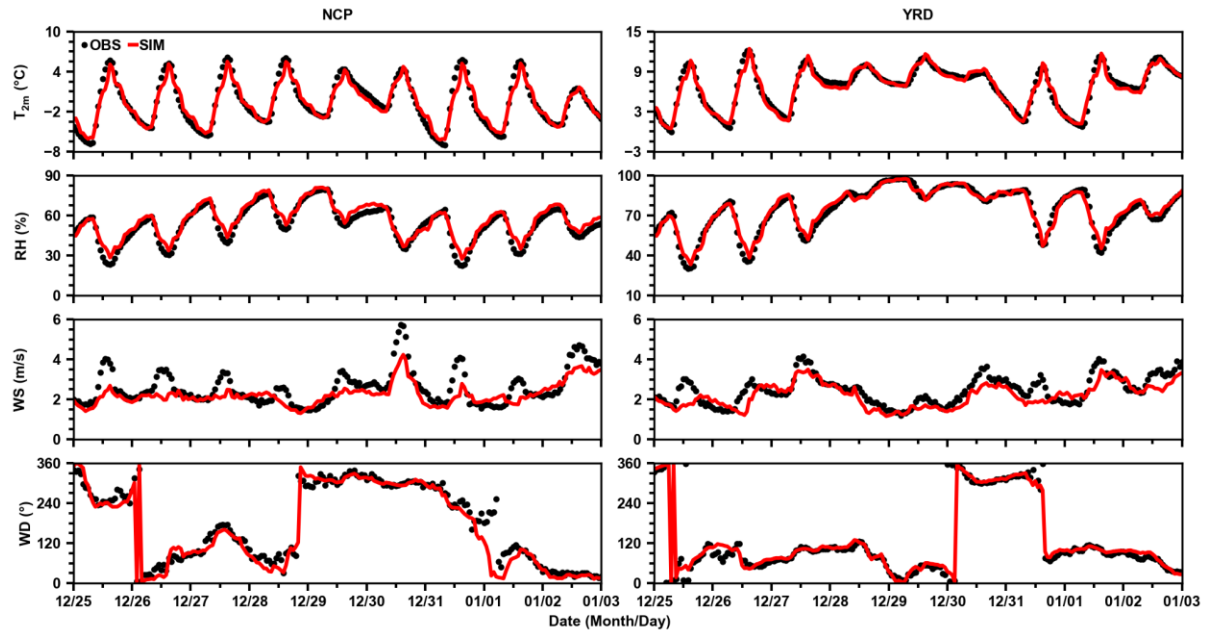


Figure S2. Time series of the observed (black dots) and simulated (red lines) hourly 2-m temperature (T_{2m} , °C), 2-m relative humidity (RH, %), 10-m wind speed (WS, $m\ s^{-1}$), and 10-m wind direction (WD, °) at NCP and YRD during December 25, 2017 to January 2, 2018.

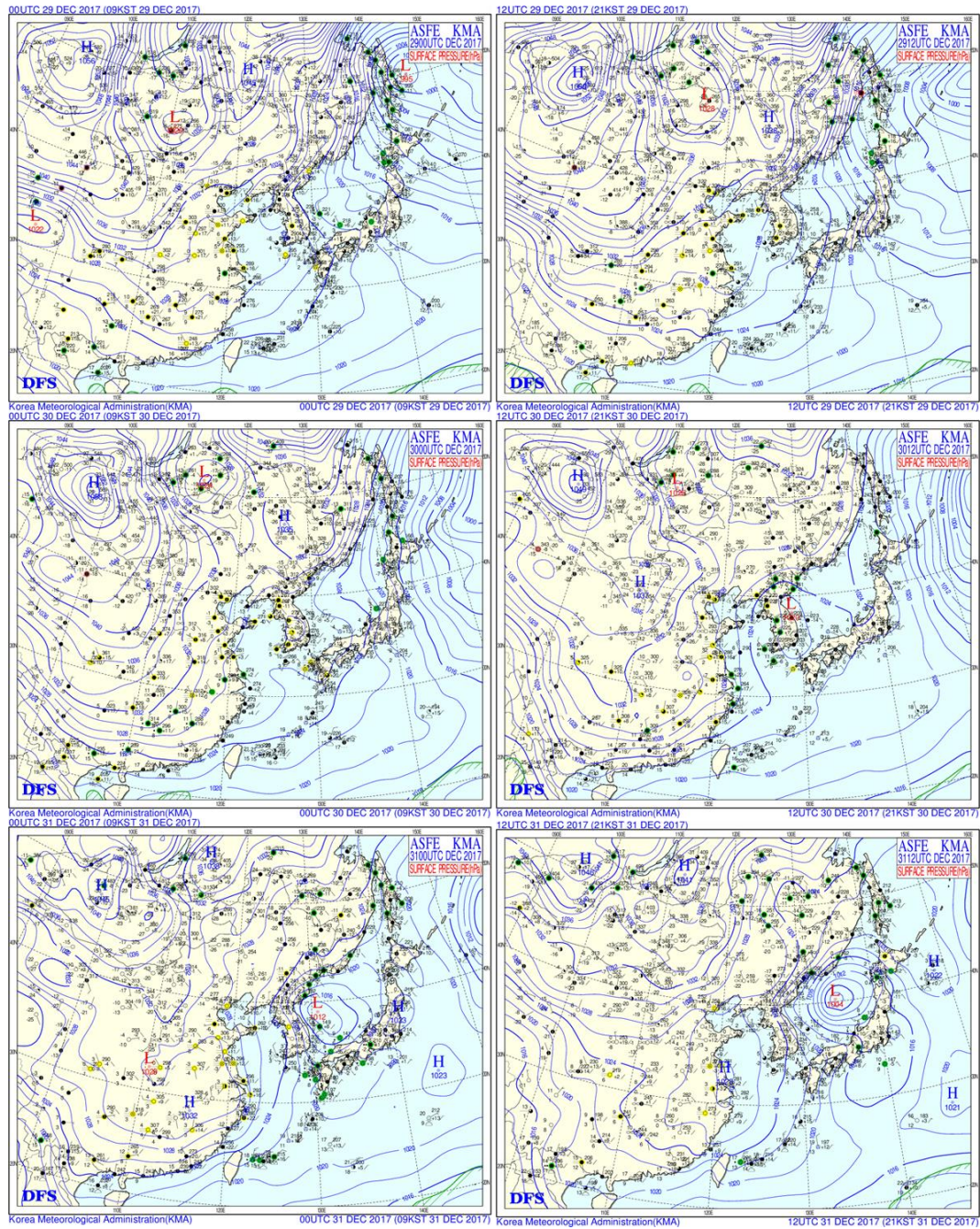


Figure S3. Surface weather pattern provided by the Korea Meteorological Administration (KMA; <http://web.kma.go.kr/chn/weather/images/analysischart.jsp>) over eastern Asia at 08:00, 20:00 LT 29–31 December 2017.

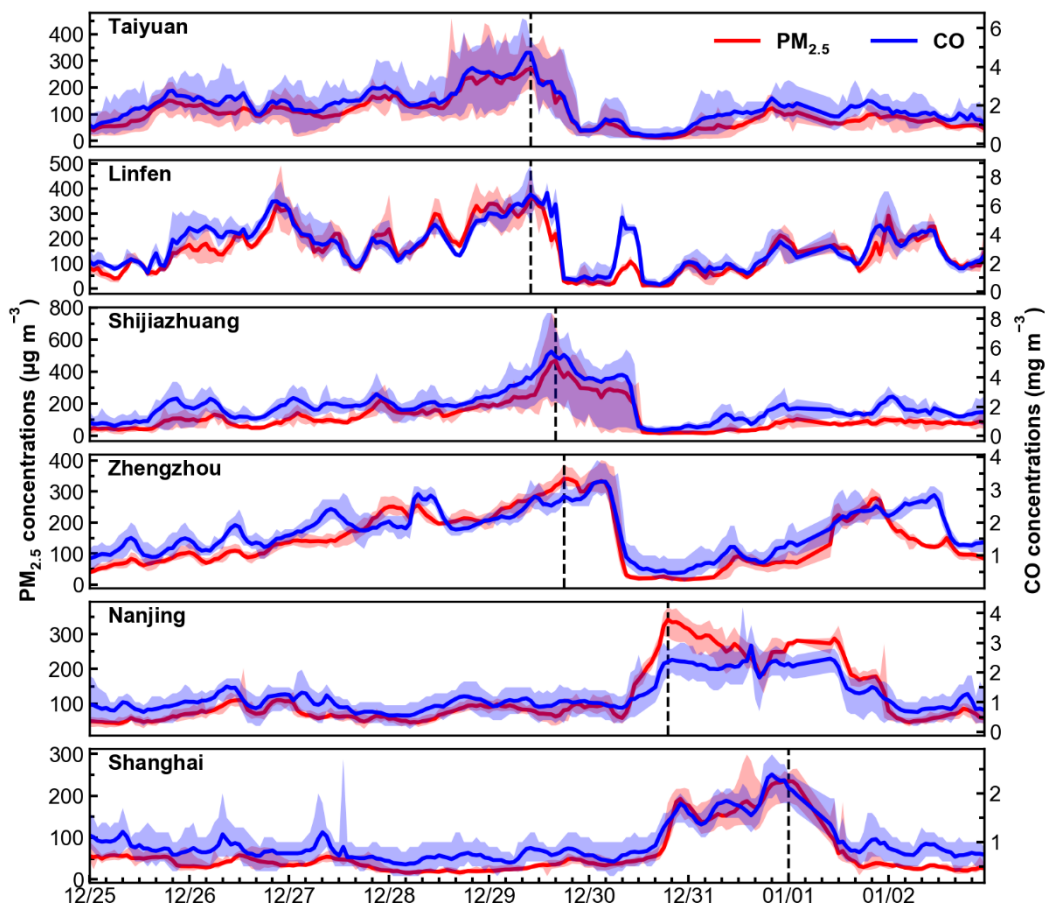


Figure S4. Time series of PM_{2.5} (red lines) and CO (blue lines) concentrations in Taiyuan, Linfen, Shijiazhuang, Zhengzhou, Nanjing, and Shanghai. Shaded areas indicate the minimum–maximum range. Black dotted lines mark the peak PM_{2.5} concentrations.

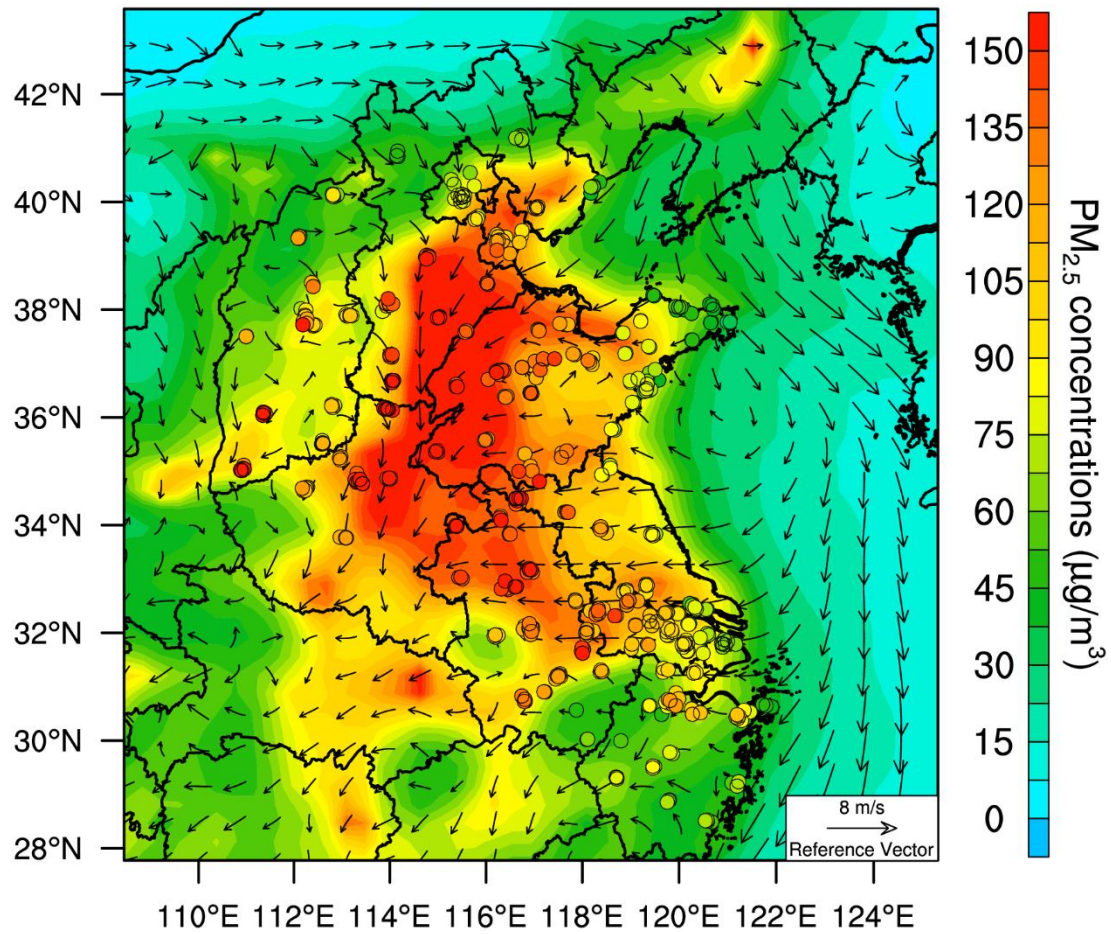


Figure S5. Spatial distribution of observed (circles) and simulated (shaded areas) episode-averaged PM_{2.5} concentrations and the WRF-simulated 10-m wind fields over eastern China from December 25, 2017 to January 2, 2018.

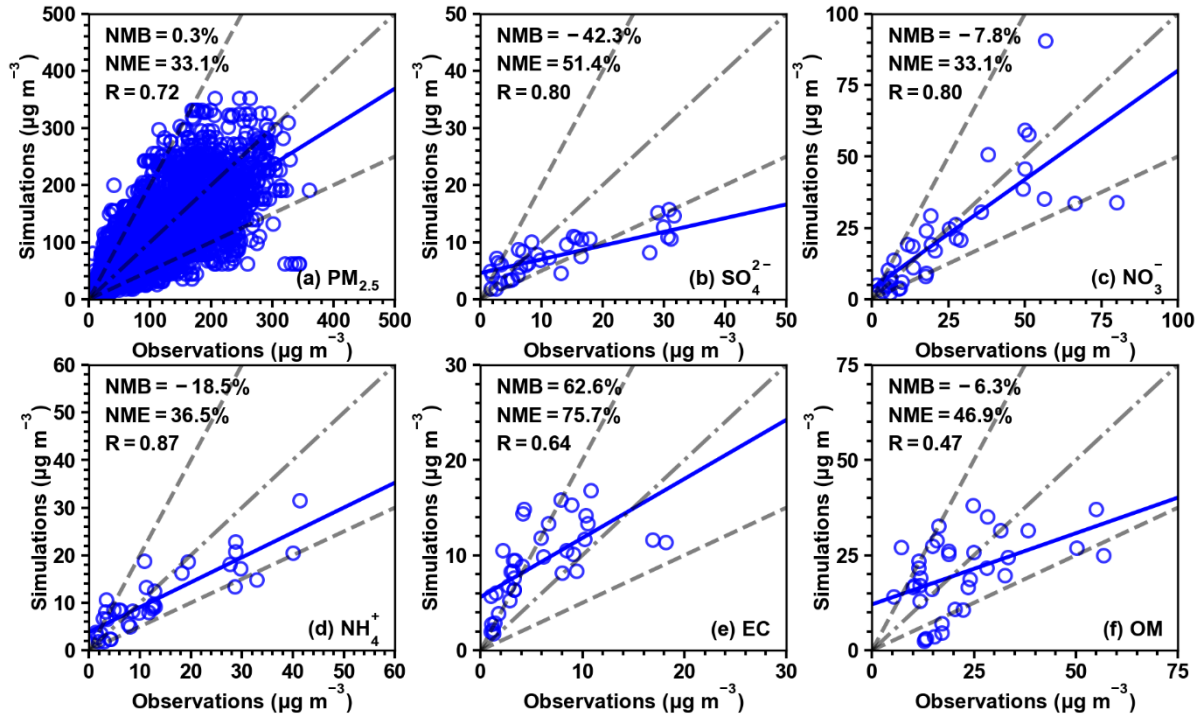


Figure S6. Scatter plots of simulated daily mean $\text{PM}_{2.5}$ in eastern China and its major chemical compositions (SO_4^{2-} , NO_3^- , NH_4^+ , EC, and OM) in Beijing, Jinan, Nanjing, and Shanghai versus observed values from 25 December 2017 to 2 January 2018.

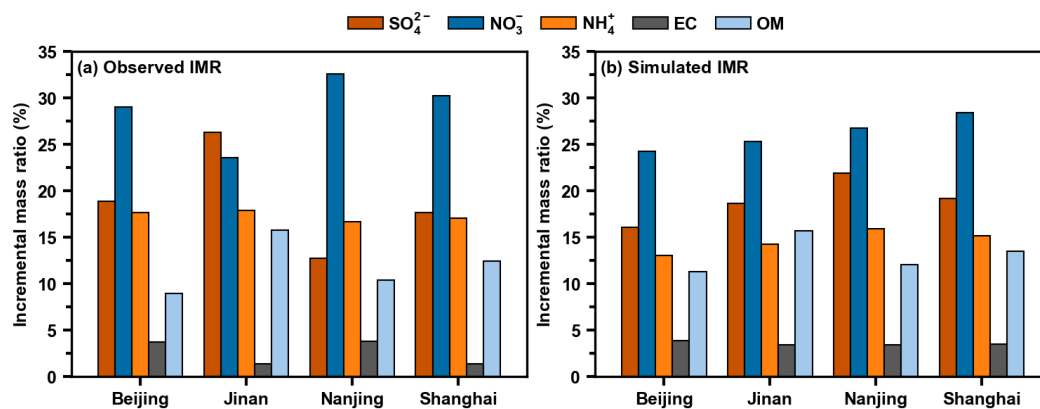


Figure S7. Comparison of the observed (a) and simulated (b) incremental mass ratio of the major PM_{2.5} chemical compositions (SO₄²⁻, NO₃⁻, NH₄⁺, EC, and OM) in Beijing, Jinan, Nanjing, and Shanghai.

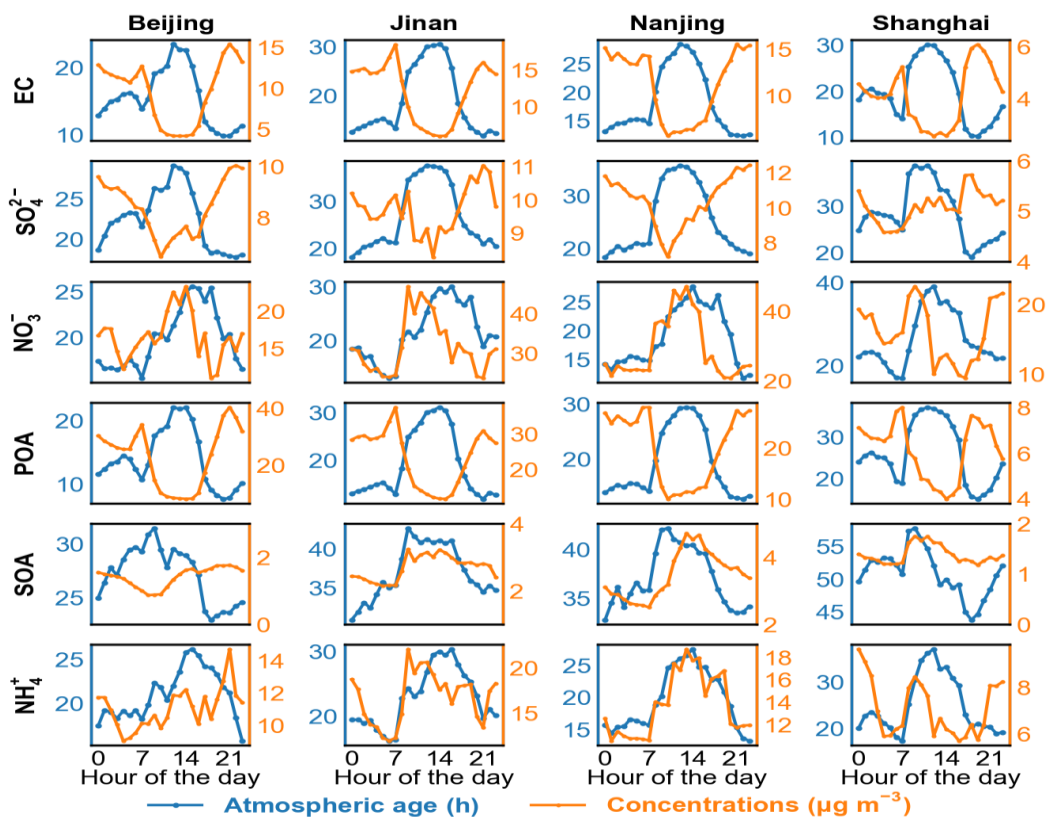


Figure S8. Diurnal variation of the mean atmospheric age and the mass concentrations of EC, SO_4^{2-} , NO_3^- , POA, SOA, and NH_4^+ in Beijing, Jinan, Nanjing, and Shanghai.

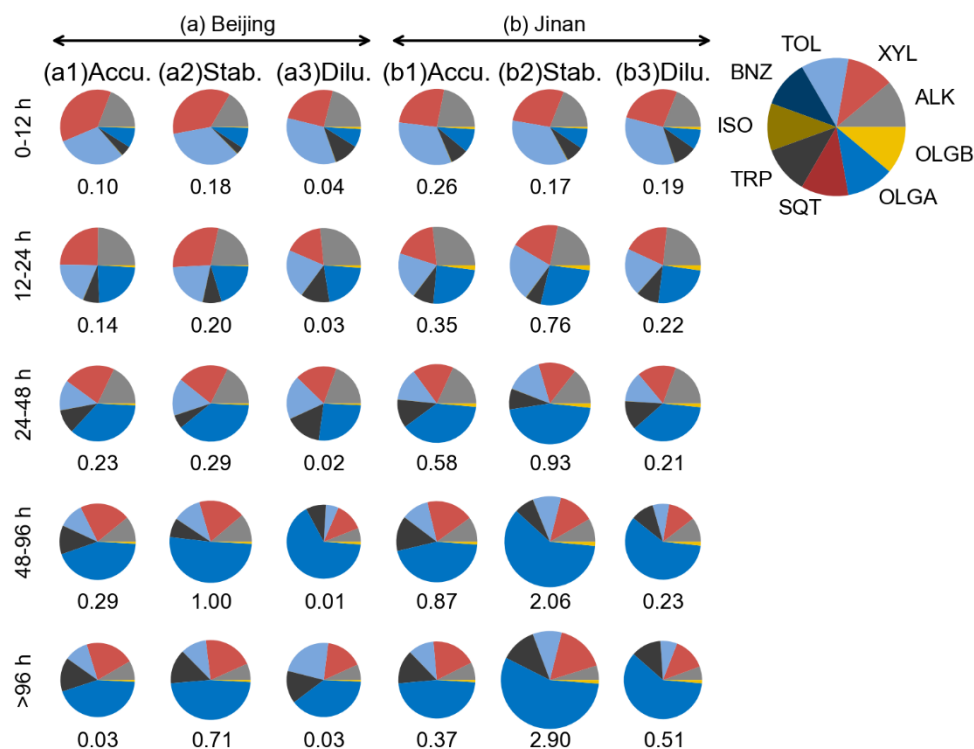


Figure S9. Fractional component contributions to SOA in different age bins in Beijing and Jinan. Accu., Stab., and Dilu. indicate the accumulation, stabilization, and dilution stage. ALK, XYL, TOL, BNZ, ISO, TRP, SQT, OLGA, and OLGB represent long-chain alkanes, xylene, toluene, benzene, isoprene, monoterpenes, sesquiterpenes, oligomers of anthropogenic SOA, and oligomers of biogenic SOA, respectively.

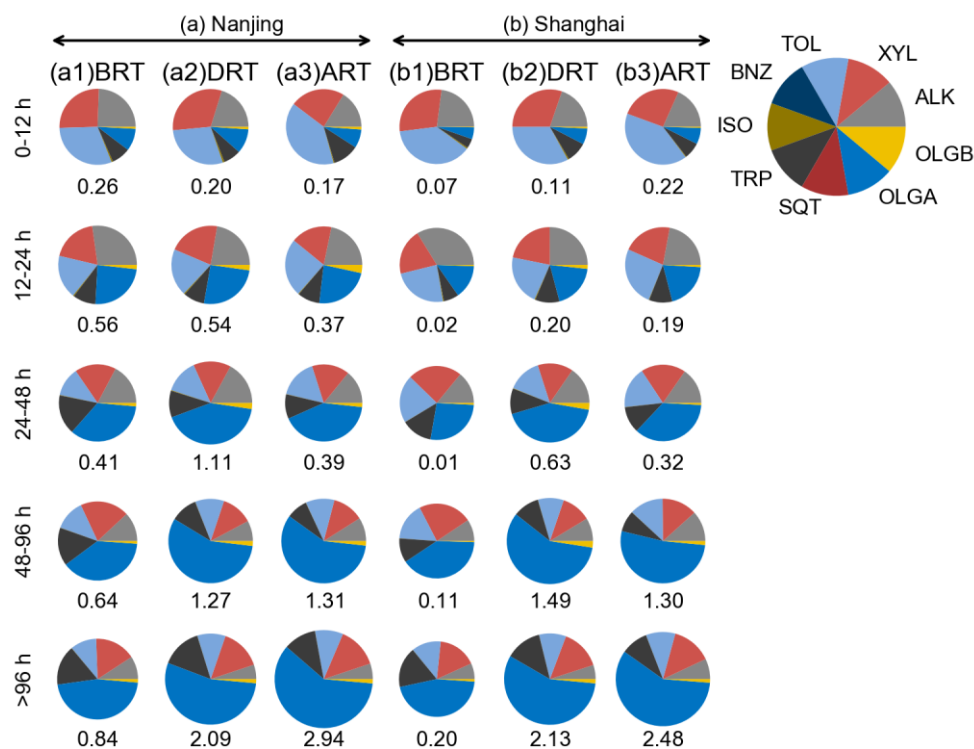


Figure S10. Fractional component contributions to SOA in different age bins in Nanjing and Shanghai. BRT, DRT, and ART indicate the period before, during, and after regional transport. ALK, XYL, TOL, BNZ, ISO, TRP, SQT, OLGA, and OLGB represent long-chain alkanes, xylene, toluene, benzene, isoprene, monoterpenes, sesquiterpenes, oligomers of anthropogenic SOA, and oligomers of biogenic SOA, respectively.

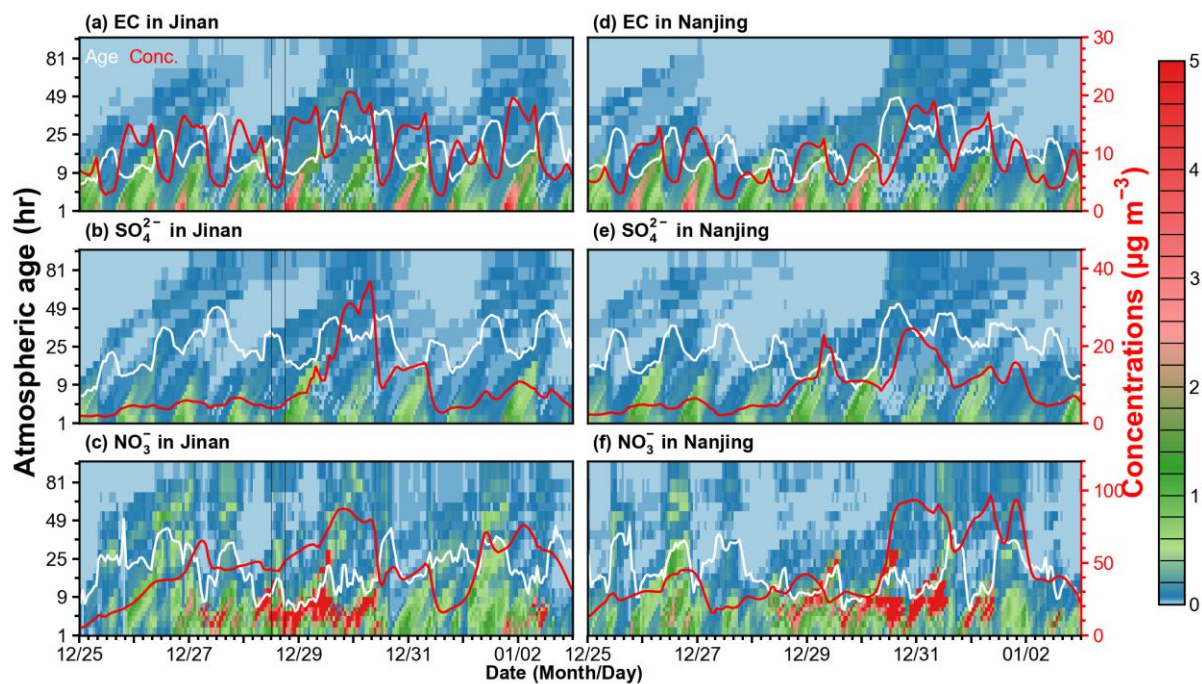


Figure S11. Hourly atmospheric age distribution of EC, SO_4^{2-} , and NO_3^- in Jinan and Nanjing during this haze episode. White lines represent the average atmospheric age, and red lines (right y-axis) indicate total mass concentrations. The results were combined from simulations with age-bin updating intervals of 1, 3, 6, 8, and 12 h. The black lines in (a–c) indicate 12:00 to 18:00 LT 28 December.

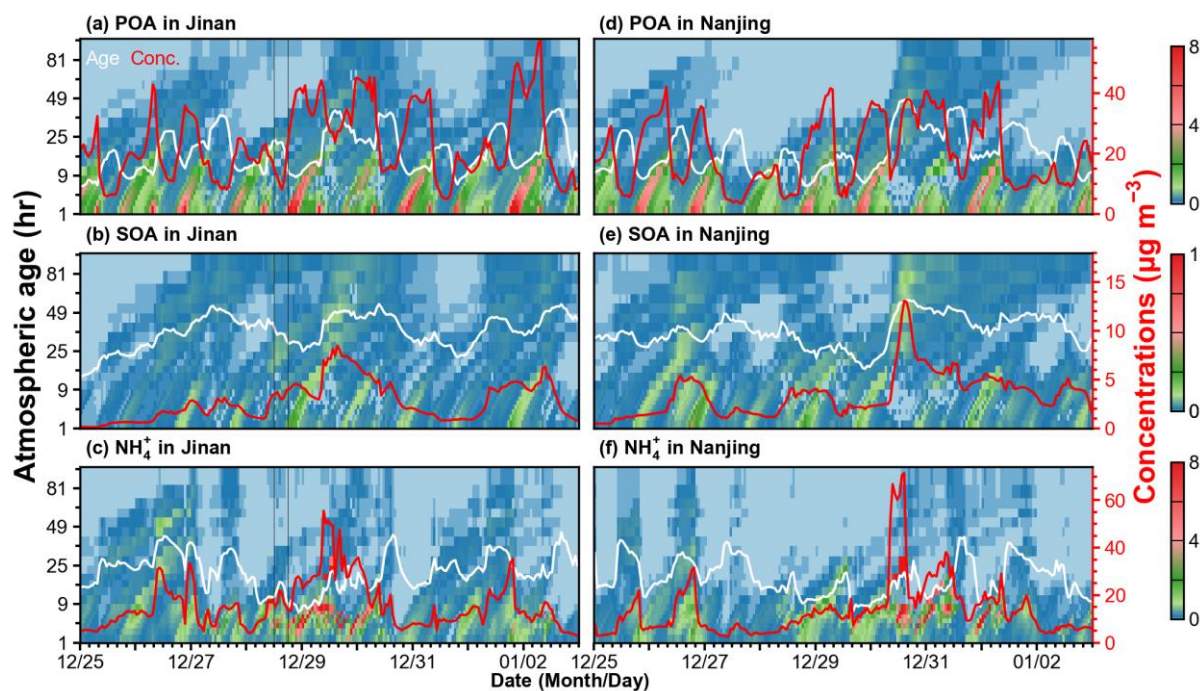


Figure S12. Hourly atmospheric age distribution of POA, SOA, and NH_4^+ in Jinan and Nanjing during this haze episode. White lines represent the average atmospheric age, and red lines (right y-axis) indicate total mass concentrations. The results were combined from simulations with age-bin updating intervals of 1, 3, 6, 8, and 12 h. The black lines in (a–c) indicate 12:00 to 18:00 LT 28 December.

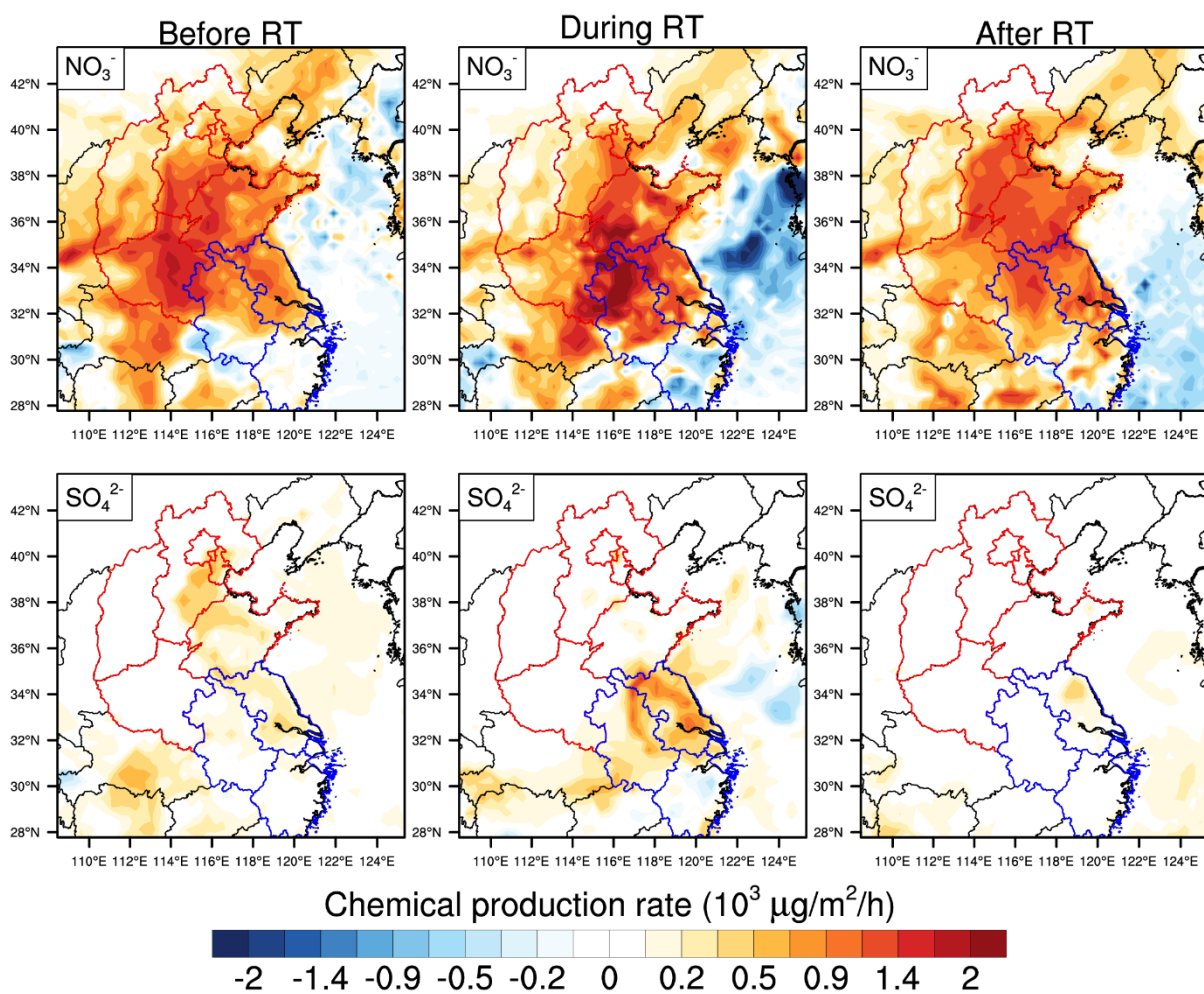


Figure S13. Spatial distribution of the averaged column chemical production rates ($\times 10^3 \mu\text{g}/\text{m}^2/\text{h}$) of NO_3^- and SO_4^{2-} before, during, and after regional transport.

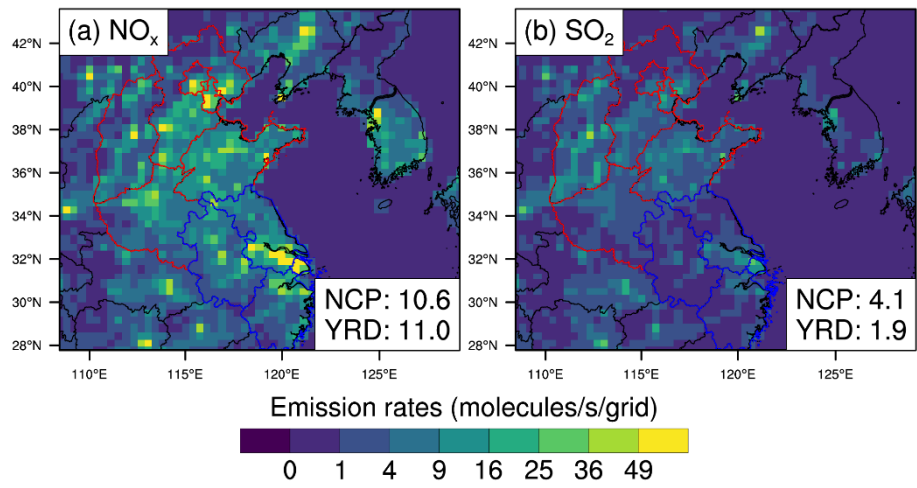


Figure S14. Spatial distribution of the emission rates (molecules/s/grid) of NO_x , SO_2 . Numbers inset each panel are the mean emission rates averaged for different regions.

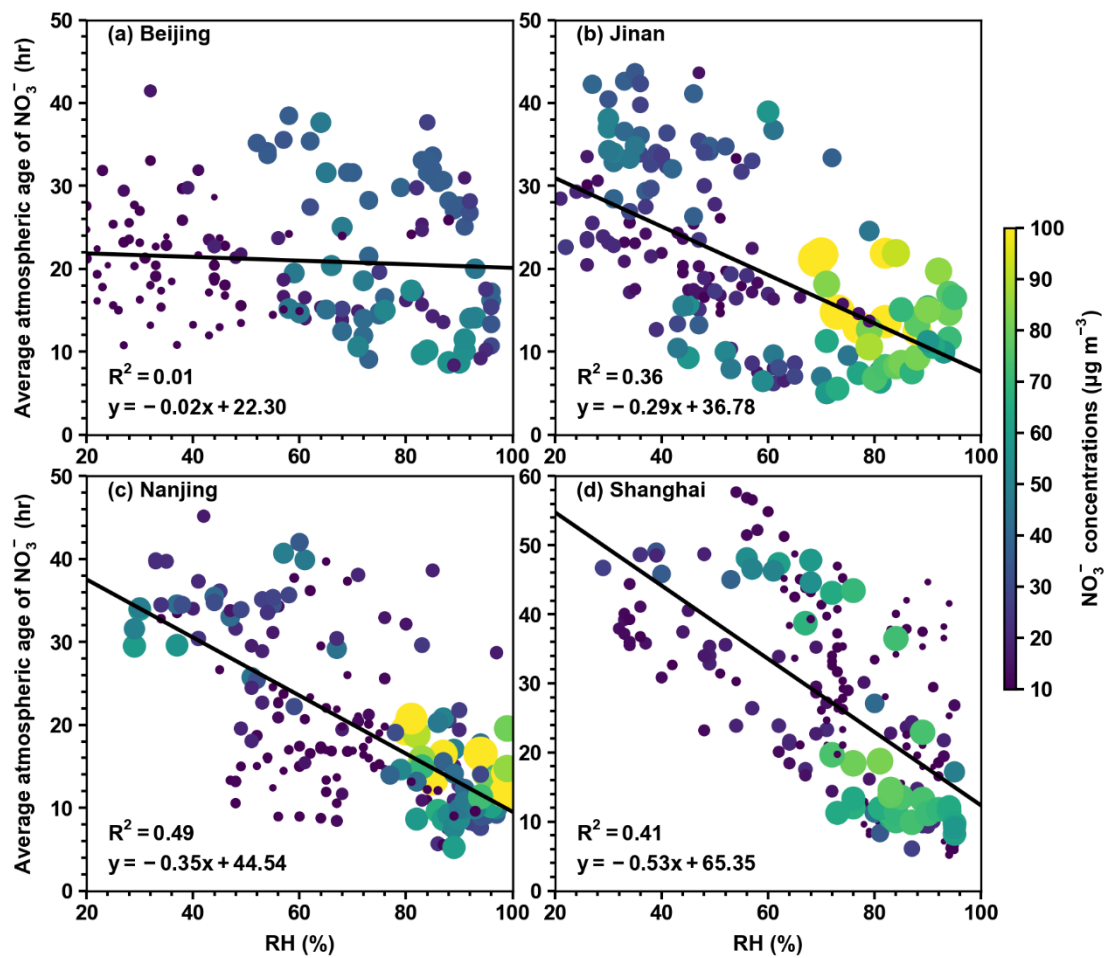


Figure S15. Average atmospheric age of NO_3^- as a function of RH in Beijing, Jinan, Nanjing and Shanghai.

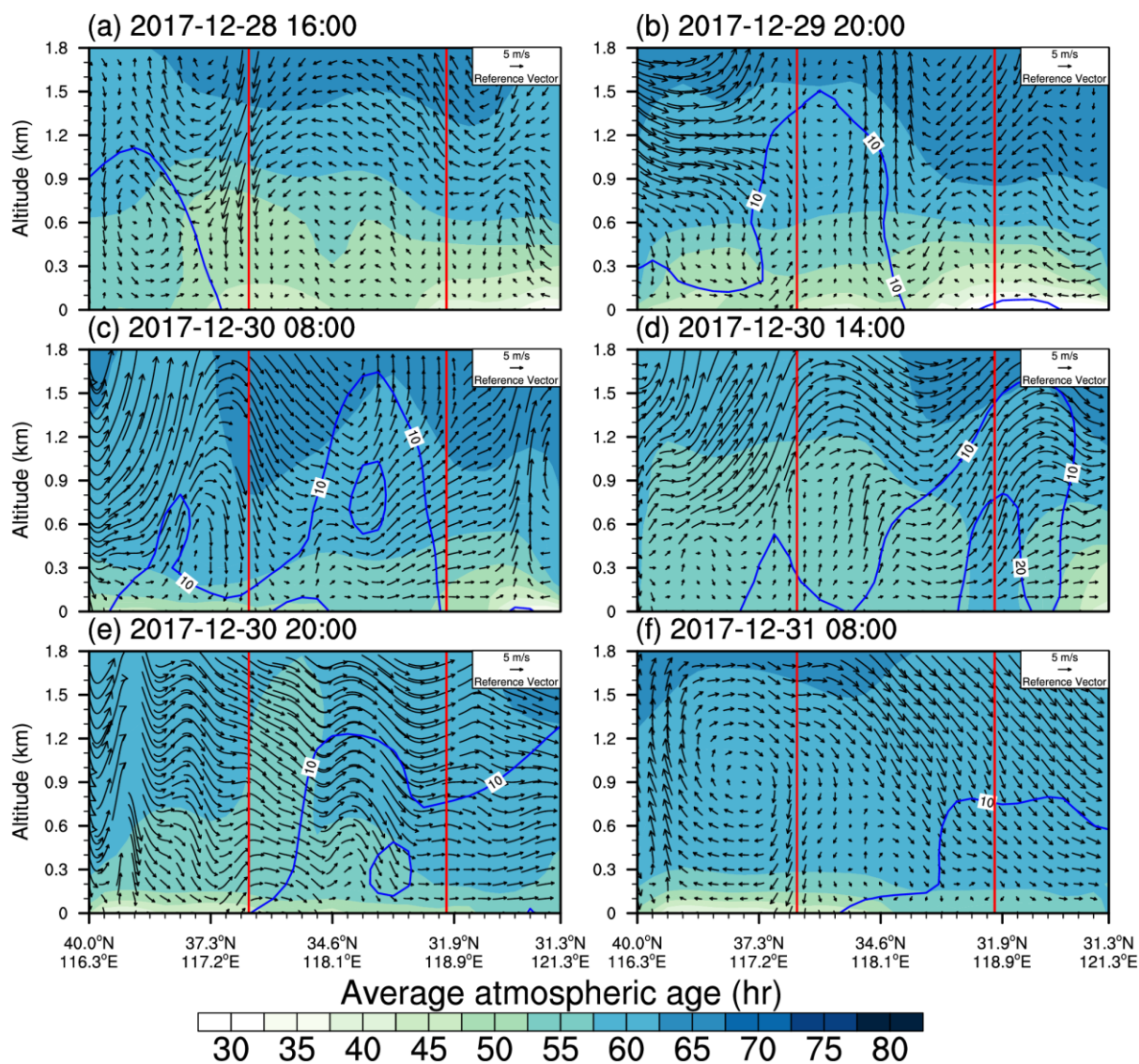


Figure S16. Vertical cross section of the average atmospheric age (color contours; h) and concentrations (blue solid lines; $\mu\text{g m}^{-3}$) of SO_4^{2-} along the transport route from Beijing to Shanghai (see white solid lines in **Figure 1**) at (a) 16:00 LT 28 December, (b) 20:00 LT 29 December, (c–e) 08:00, 14:00, 20:00 LT 30 December, and (f) 08:00 LT 31 December 2017. Note that the vertical wind speed was multiplied by 500 for the illustration of vertical circulations. The location of Jinan and Nanjing are marked as red solid lines.

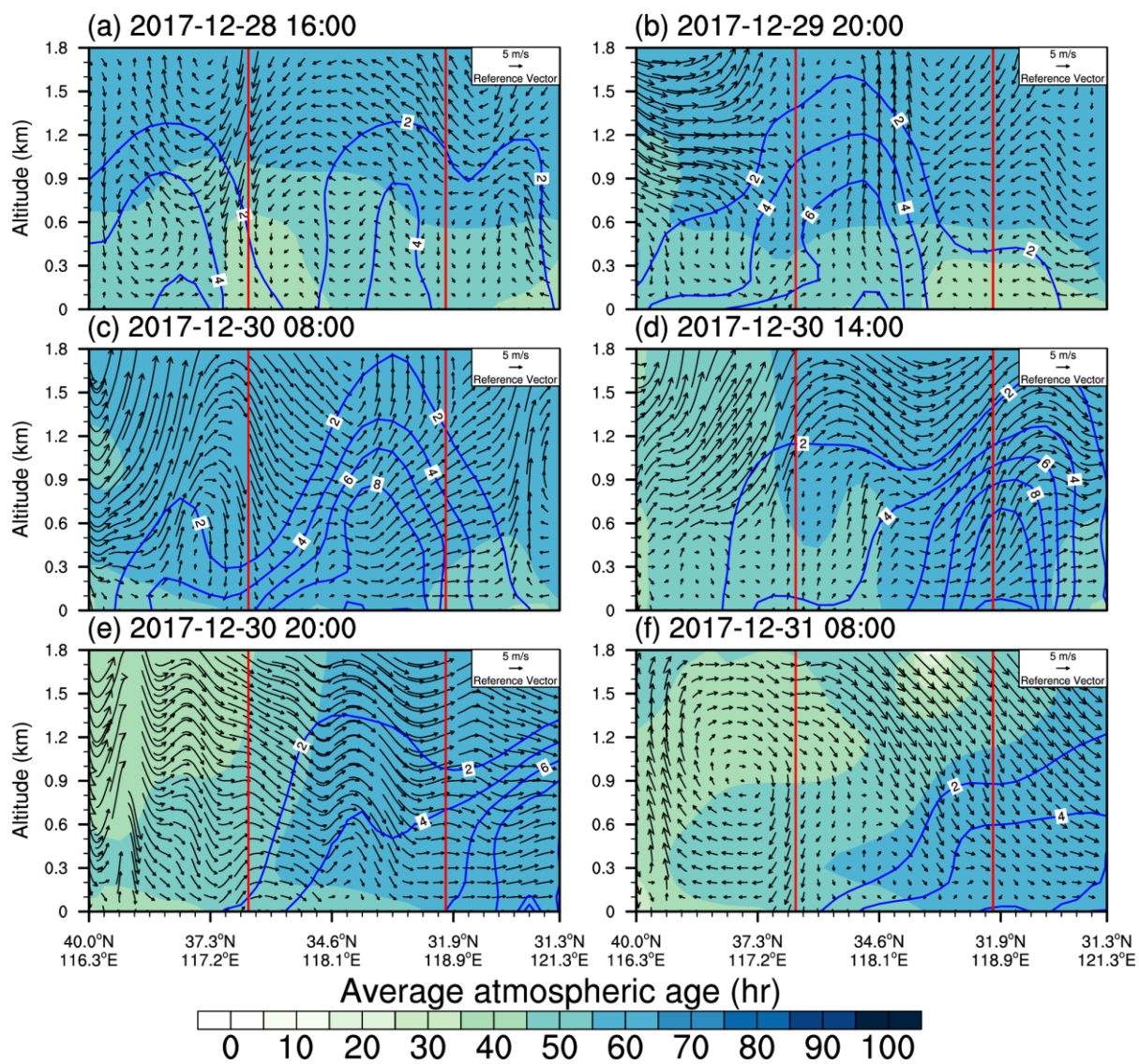


Figure S17. Same as Figure S16 but for SOA.

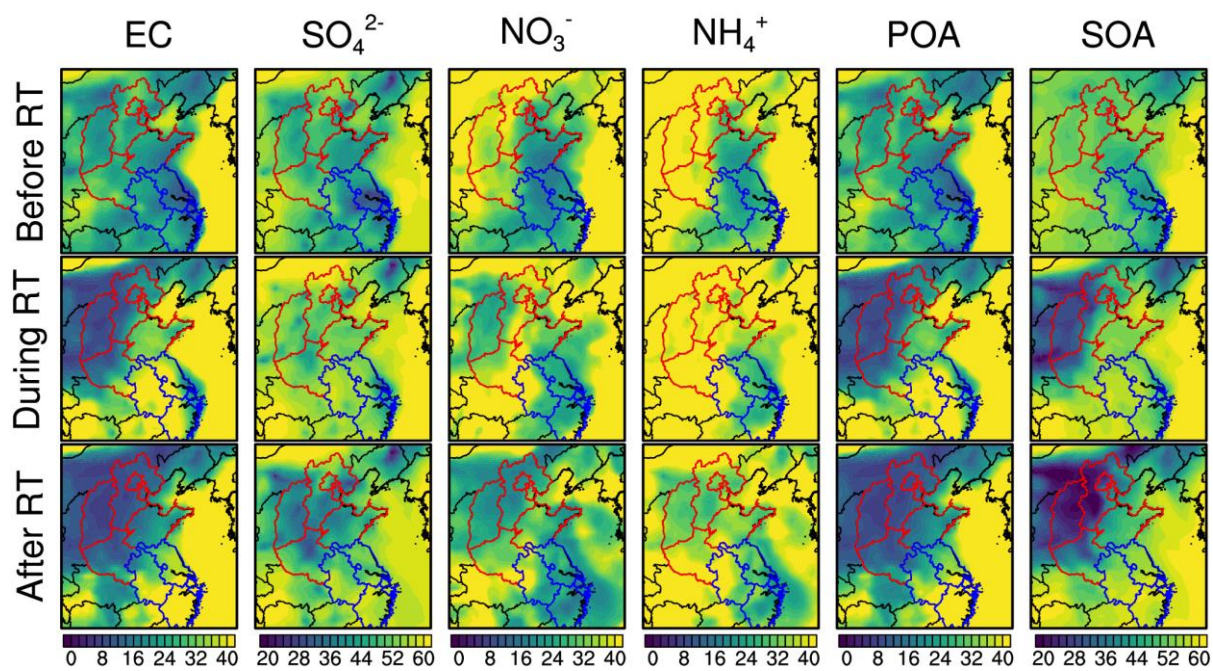


Figure S18. Spatial distribution of the mean atmospheric age of EC, SO_4^{2-} , NO_3^- , NH_4^+ , POA, and SOA on ground level before, during, and after the regional transport. Units are hours.

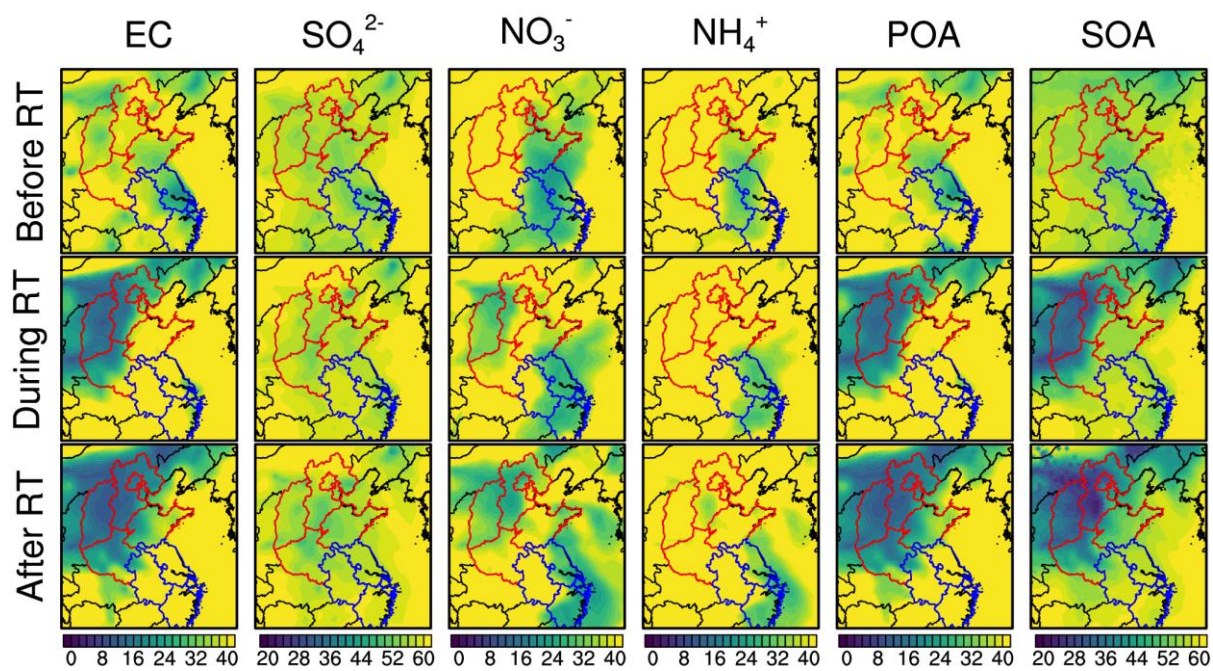


Figure S19. Spatial distribution of the mean atmospheric age of EC, SO_4^{2-} , NO_3^- , NH_4^+ , POA, and SOA averaged vertically before, during, and after the regional transport. Units are hours.

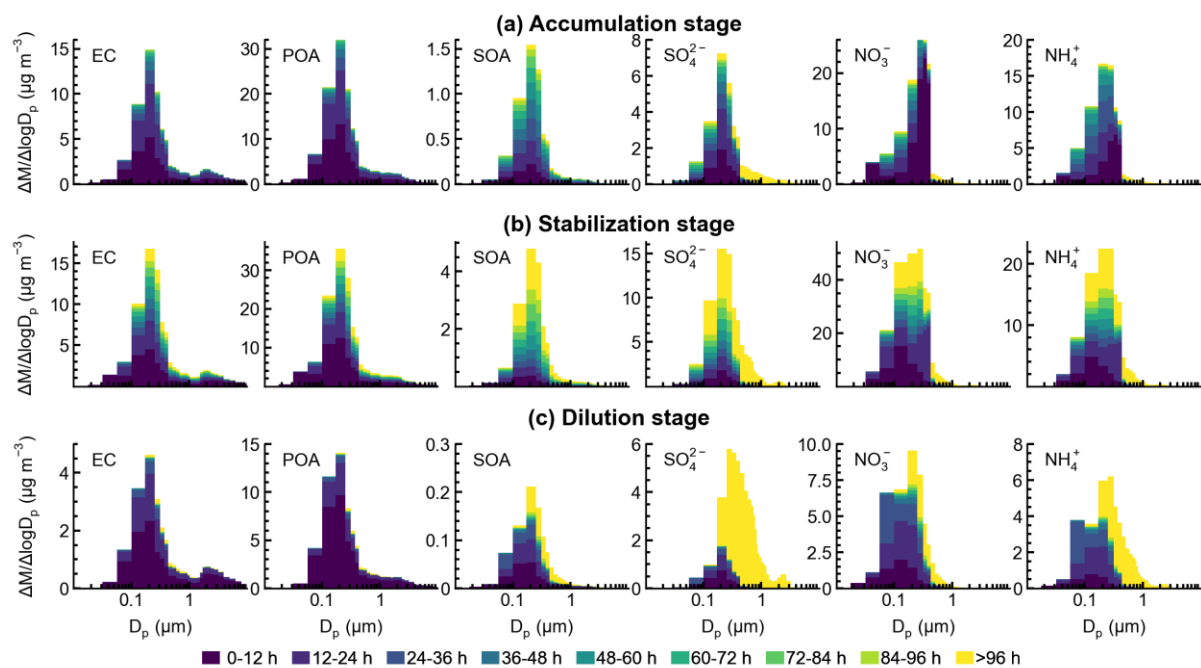


Figure S20. The size distribution of EC, POA, SOA, SO_4^{2-} , NO_3^- , and NH_4^+ in Beijing during (a) accumulation stage, (b) stabilization stage, and (c) dilution stage.